Green Synthesis Derived CdS Quantum Dots Using Tea Leaf Extract: Antimicrobial, Bioimaging and Therapeutic Applications in Lung Cancer Cell

Kavitha Shivaji,[a] Suganya Mani,[a] Ponmurugan Ponnusamy,[b] Catherine Suenne De Castro,[c] Matthew Lloyd Davies,[c] Mythili Gnanamangai Balasubramanian,[a] Sudhagar Pitchaimuthu,[c]**

a. Department of Biotechnology, K.S.Rangasamy College of Technology, Tiruchengode. 637215, Tamil Nadu. INDIA.

b. Department of Botany, Bharathiar University, Coimbatore 641 046, India

c. SPECIFIC, Materials Research Centre, College of Engineering, Swansea University (Bay Campus), Fabian Way, Swansea SA1 8EN, United Kingdom.

KEYWORDS: Green synthesis; CdS QDs; *Camellia* sinensis extract; antimicrobial activity; bioimaging; A549 cell; apoptosis; flow cytometer.

ABSTRACT

Low dimensional semiconductor quantum dots (<10 nm) have received great attention for potential use in biomedical applications (diagnosis and therapy) for which larger nanoparticles (>10 nm) are not suitable. Here, we demonstrate a green, biogenic synthesis route for making CdS quantum dots (QDs) with 2-5 nm particle size using tea leaf extract (*Camellia* sinensis) as a toxic-free particle stabilizing agent. We have explored the biological activity of these CdS QDs in different applications, namely; a) antibacterial activity b) bioimaging and c) apoptosis of lung cancer cells. The antibacterial activity of the CdS QDs has been studied against different types of bacteria growth, showing that CdS QDs effectively inhibit the bacterial growth and exhibit cytotoxicity towards A549 cancer cells when compared to a control (no QD treatment). We have compared this cytotoxicity effect on A549 cancer cells with a standard drug, cisplatin, showing comparable results. Additionally, these CdS QDs produce high contrast fluorescence images of A549 cancer cells indicating a strong interaction with the cancer cell. To further understand the role of CdS QDs in bioimaging and cytotoxicity effect in A549 cells, fluorescence emission and flow cytometry analysis were carried out. The fluorescence emission of CdS QDs were recorded with λ_{exc}= 410 nm, showing concentration dependence fluorescence emission centered at 670 nm. From the flow cytometry analysis, it is confirmed that the CdS QDs are arresting the A549 cell growth at the S phase of cell cycle, inhibiting further growth of lung cancer cell. The multifunctional advantages of *Camellia sinensis* extract mediated green CdS QDs will be of widespread interest in implementing *in-vivo* based bioimaging and therapeutic cancer treatment applications.

Introduction

Low dimensional semiconductor nanoparticles and/or quantum dots (QDs) have received great attention in cancer treatment nanotechnology. For instance, as-synthesized or modified nanoparticles are widely applied in tumor imaging, drug delivery[1,2] and diagnosis and treatment of cancer[3,4]. In this context, low dimensional nanomaterials based nano-formulated drugs are promising candidates to treat disease via targeted drug delivery[5,6]. Targeted drug delivery based biological treatment is highly precise and prevents side effects originating from systemic distribution of cytotoxic drugs and effectively controls cancer cell proliferation or tumor angiogenesis[7-8].

Recent reports show that metal based nanoparticles can efficiently destroy cancerous cells [9, 10, 11, 12]. In particular quantum dots (QDs), show superior production of reactive oxygen species (ROS) in biological systems [10, 13, 14]. In addition, QDs have other advantages including; typical sizes of <10 nm, exceptional physicochemical properties, low cytotoxicity and bio-compatibility. Thus, semiconductor QDs have found use in a number of biomedical applications, including bio-imaging, bio-sensing and drug delivery [15, 16, 17, 18, 19, 20, 21,22]

CdS QDs have been identified as a potential candidate to diagnose cancerous cells.[23] CdS QDs have been synthesized through a broad range of physical and chemical techniques such as microwave heating, micro emulsion synthesis and ultrasonic irradiation [24, 25]. However, for highly precise detection of cancer cells, CdS QDs made from standard chemical synthesis is complicated and expensive, requiring hazardous chemicals and multiple synthetic steps[26]. Therefore, alternative approaches are needed which allow synthesis using non-hazardous materials, whilst maintaining the important properties of size, physicochemical properties, low cytotoxicity and bio-compatibility. In this context, nanoparticles made via biogenic synthesis using bio-surfactants (microbes and plants) are a promising approach. Also, it offers precise control of the particle size distribution and homogeneity through a slow rate of chemical

reaction.[27] Compared to conventional chemical based particle stabilizers, plant extract based surfactants exhibit many advantages such as biodegradability, biocompatibility and low-toxicity[28, 29, 30, 10] . Borovaya *et al* [31] reported *Nicotinum tabaccum* act as a biological source for quantum dots synthesis to produce biocompatible QDs. In addition, microorganisms such as bacteria, fungi and yeast have also been studied for biogenic synthesis of nanomaterials. For instance, *Bacilllus licheniformis* is a microbial source for synthesis of gold nanotubes [32]. Moreover, there have been a few studies of water soluble QDs which have been reported but they have needed expensive precursors for their production[33]. Galeone *et al* [34] demonstrated different polymer coated CdS quantum dots showing appreciable biocompatibility. Recent reports on CdS QDs derived from biogenic synthesis [35] show excellent quantum confinement effect [36], high luminescence emission [31, 37] and excellent antimicrobial activity[38]. One of the main advantages of biogenic synthesis approach is that organic biomolecules from plant extracts are involved as a stabilizing agent to control the particle size of the CdS QDs which does not induce any significant damage to the cells [24, 31]. Recent studies on *Asparagus racemosus* extract mediated CdS quantum dots showed less DNA damage activity [39]. This highlights that plant extract mediated CdS QDs can be biocompatible, less toxic and cost effective and thus highly promising for *in vitro* studies.

In this context, we have derived CdS QDs using tea leaf (*Camellia sinensis)* extract as particle stabilizing agents. Tea leaves contain polyphenols, amino acids, caffeine, vitamins, minerals and antioxidants. It is anticipated that chemical constituents of *Camellia sinensis* plays a key role in the formation of CdS QDs. For the first time, we demonstrate the biological activity (antibacterial, intracellular fluorescence mapping, apoptosis effect on A549 cells) of *Camellia sinensis* derived CdS QDs. This work highlights the synthesis of low dimensional green semiconductor QDs and explores the inter-relationship between material property and

biological activity (antibacterial, hemolytic activity and anticancer activity in lung cancer cells). The results were compared with control samples and commercial products.

EXPERIMENTAL SECTION

Materials: Cadmium sulfate ($CdSO_4$, 99.99% purity) and sodium sulfide (Na_2S, 98 % purity) were obtained from sigma Aldrich, USA. All other reagents were used in analytical grade. Deionized water used throughout experiment obtained from ultra-pure water purification system.

Preparation of plant extract: The *Camellia sinensis* plant leaves were obtained from Valparai (Tamil Nadu, India) location. First, the leaves were washed with distilled water and then dried under shade. Followed that 3 g of chopped leaves were taken, with 30 mL of methanol and kept at 24 h incubation. Then the extract solution was filtered through the Whatman qualitative filter paper (grade number 1) and stored at 4℃ for further use.

Green synthesis of CdS quantum dots: The CdS QDs were prepared in two stages. In first stage 2 mL of 0.025 M $CdSO_4$ was added to 30 mL of *Camellia sinensis* extract and kept for 3 days incubation in the dark. In the second stage, 0.5 mL of 0.025 M Na_2S was added and incubated for another 4 days to produce CdS nanoparticles. The resultant final solution was in bright yellow colour and was centrifuged at 13,000 rpm for 10 minutes. In order to remove the contamination in the recovered CdS QDs, the solid was washed with deionized water and repeated three times. Finally, the pellet was lyophilized for further characterization studies. The experimental stages of CdS QDs is illustrated in Scheme 1.

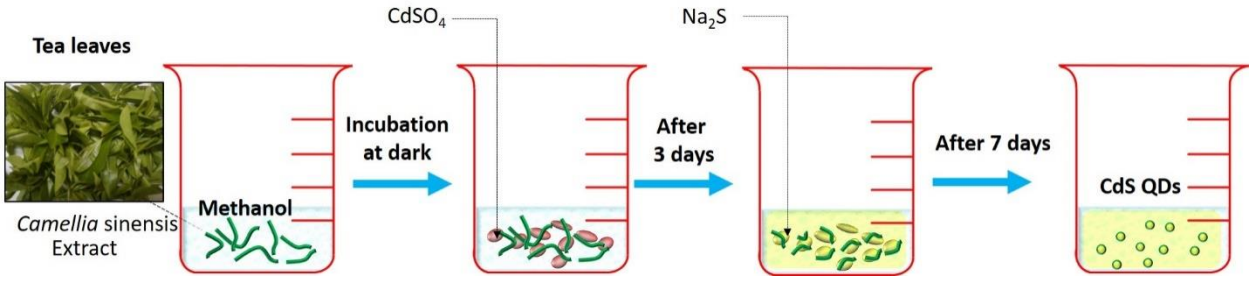

Scheme 1. Illustration of experimental stages involved in *Camellia sinensis* extract mediated green CdS QDs synthesis.

Measurements and analysis: The surface morphology and elemental analysis of resultant CdS solid sample was recorded using scanning electron microscope SEM (JEOL JSM 6360, Japan) coupled with EDX (Oxford instrument, INCApentaFETx3, England). Further, shape, and crystalline nature of the resultant CdS solid sample was studied using high resolution transmission electron microscopy (HRTEM) (JEOL JEM 2100, Japan). In order to understand the influence of organic species presence in the plant extract on CdS the FTIR spectra was recorded with a resolution of 1 cm^{-1} in the transmittance mode and 100 mg of potassium bromide (KBr) used as a reference (IR prestige 21, Shimadzu). The UV-Vis absorption and fluorescence emission spectra were performed on a Perkin Elmer Lambda 9 and a Horiba FluoroMax-4, respectively. The excitation wavelength was selected via monochromator and no filter was added on the pathway. For optical measurements, the CdS QDs were dispersed in ethanol and DMSO solvent.

Biological studies:

Antibacterial activity: Antibacterial activity of CdS QDs is studied by well diffusion method against *Escherichia coli*, *Serratia marcescens*, *Streptococcus pyogens*, *Staphylococcus aureus* and *Klebsiella pneumoniae*. The clinical pathogenic cultures were inoculated in nutrient broth and incubated for overnight at shaking incubator (37°C). The overnight grown bacterial culture was swabbed on Muller Hinton agar with sterile cotton swabs. A 5 mm diameter of well was made on agar plates. In these wells, different concentrations of CdS QDs (40, 80, 120, 160 and

200 µg/mL) were loaded and incubated for 24 hours. After incubation period, the zone of inhibition was measured with millimeter ruler.

Hemolysis activity: The process of hemolysis was used for determining toxic effect of the drug with RBC cells. Healthy human blood sample was freshly harvested and PBS (phosphate buffer saline, pH 7.4) was added at 1:2 volume ratio. Further, it was centrifuged at 10,000 rpm for 15 minutes. Finally, RBCs (red blood cells) were isolated by removing the supernatant. In order to remove erythrocytes from the RBCs it washed with sterile PBS for five times. The resultant RBC cells were diluted with 40mL of PBS. Then 0.2 mL of RBC cells at different concentrations of CdS QDs (10, 20, 30, 40, 50 and 60 µg/mL) were mixed to RBC cells in vortex. These samples were incubated at room temperature (24℃) for 3 hours. Then centrifuged at 10,000 rpm for 2 minutes, the supernatant was finally taken out for recording optical absorbance analysis at 541 nm[40] wavelength. The percentage of hemolysis was estimated using the relation

$$Hemolysis = \frac{Sample\ \ Abs - Negative\ Control}{Postive\ Control - Negative\ Control} \times 100 \qquad (1)$$

Note that the RBC cells were incubated with water and PBS for positive and negative controls, respectively.

Cytotoxic activity: The cytotoxic effect of the resultant CdS QDs solid sample was treated with A549 cells by MTT assay. To evaluate the efficiency of CdS QDs samples, a similar cytotoxic protocol was carried out using cisplatin (standard drug). The human lung alveolar basal epithelial cell line (A549) was purchased from the National Centre for Cell Sciences (NCCS), Pune, India and cells were maintained in DMEM (Dulbecco's Modified Eagle media) medium with nonessential amino acids. The cells were maintained at 37℃ with 5% of CO_2 incubator until the growth attained 90 % confluence and cells were seeded in a 96 well plate at a density of 4×10^3 cells/well. For comparative cytotoxicity analysis, the A549 cells were treated with different concentrations of CdS QDs and standard drug cisplatin (10, 20, 30, 40 and 50

μg/mL) which incubated for 24 hr. For MTT assay analysis, 100 μl of MTT- (3-(4,5-dimethylthiazol-2-yl)-2,5-diphenyltetrazolium bromide) was added with above mentioned CdS QDs as well as cisplatin drug treated cells and kept for 4hr incubation. Then finally 100 μl of dimethyl sulphoxide (DMSO) was added which resulted in purple colour formazon crystals. The plates were read at 620 nm in a multi well plate reader (Biorad) and the percentage of cell viability is calculated by using the formula.[41]

$$\text{Percentage of viability} = \frac{\text{Absorbance of treated cells (CdS QDs)}}{\text{Absorbance of control cells (untreated)}} \times 100 \qquad (2)$$

In order to ensure morphological change in A549 cells under different concentrations of CdS QDs treatment (10, 25 and 50 μg/mL), the treated samples were grown on coverslips (1×10^5 cells per coverslip) and incubated for 24 h. Following the incubation, the samples were fixed with methanol: acetic acid solution (3:1, v/v). The resultant A549 cells grown coverslip was gently mounted on the glass slide and morphological change were recorded using a bright field microscope (Nikon, Japan) at 40x magnification.

Apoptosis Assessment: A549 cells was seeded in a six well plate and treated with different concentrations of CdS QDs (10, 25 and 50 μg/mL) for 24 hours. Then these cells were washed with phosphate buffered saline (PBS - pH 7.2) and finally stained with AO/EtBr [100 mg/mL of acridine orange (AO) and 100 mg/mL of ethidium bromide (EtBr) in deionized water. After the cells were kept at 3 minute incubation, it was visualized under fluorescence microscope (Nikon Eclipse, Inc, Japan) at 40x magnification with an excitation filter at 480 nm. The similar procedure was followed for DAPI (4',6-diamidino-2-phenylindole).[42]

Cell cycle analysis by flow cytometry: A549 cells ($1x10^5$) were seeded in a six well plate. After 24 h incubation at 37˚C (5% of CO_2), it was changed to fresh medium and supplemented with the CdS QDs (10, 25 and 50 μg/mL). After 24-h incubation, the untreated and CdS QDs treated A549 cells were harvested with trypsin. Then these samples were washed by PBS and fixed in 70% of ethanol and stored at -20˚C for 1h. The cellular nuclear DNA was stained with

propidium iodide (PI) and removing the ethanol content through PBS washing. Then cells were suspended with 0.5 mL PBS containing 50 µg/mL of PI and 100 µg/mL RNase were added and kept incubation at 37˚C for 30 min. Flow cytometry was performed in duplicate with a BD FACS flow cytometer (USA). From each sample 10,000 events were collected. The fluorescent signal intensity was recorded and analyzed by CellQuest and Modifit.

Apoptotic analysis of A549 cells: The apoptotic effect of CdS quantum dots at A549 cells (1×10^5 cells/mL) was studied through *annexin V-FITC* and *propidium iodide* dual staining flow cytometry method. After incubation period, QDs treated A549 cells were harvested, and washed with PBS. Then finally treated with Trypsin/EDTA solution and suspended cells were centrifuged at 2000 rpm for 10 mins. In the cell pellet, above mentioned 100 µl of *annexin V-FITC* (Strong Biotech Co., Taipei, Taiwan) staining solution was added and incubated for 15 minutes at 25℃. These cells were then analyzed with a flow cytometer (FACS verse, BD Bioscience, USA).

Statistical analysis: All the *in vitro* experiments were carried out in triplicate and the experiments repeated at least three times. Statistical analysis was performed by one-way ANOVA (GraphPad Prism 5.0 software), followed with Bonferroni test for multiple comparisons. Statistical evaluation is performed using the results from a mean standard deviation of three experiments in each batch.

RESULTS AND DISCUSSION

Structural analysis: **Figure 1 (a)** and **(b)** show the surface morphology and composition analysis of the as-synthesized CdS sample. From **Figure 1a**, SEM image depicts smooth and spherical morphology of the CdS particles. The strong peaks from energy dispersion spectra (EDS) corresponding to Cd and S indicating the formation of cadmium sulfide (**Figure 1b**). The additional oxygen peak presence in the EDS spectra might originate from organic capping

material bound on the surface. The similar observation on presence of oxygen species from biosynthesized CdS using *Chlamydomonas reinhardtii* is reported in the literature.[43] Furthermore, the shape and particle size of the CdS particles were studied by HRTEM. **Figure 1c** demonstrates that the CdS particles are homogeneously distributed in the range from 3-5 nm.

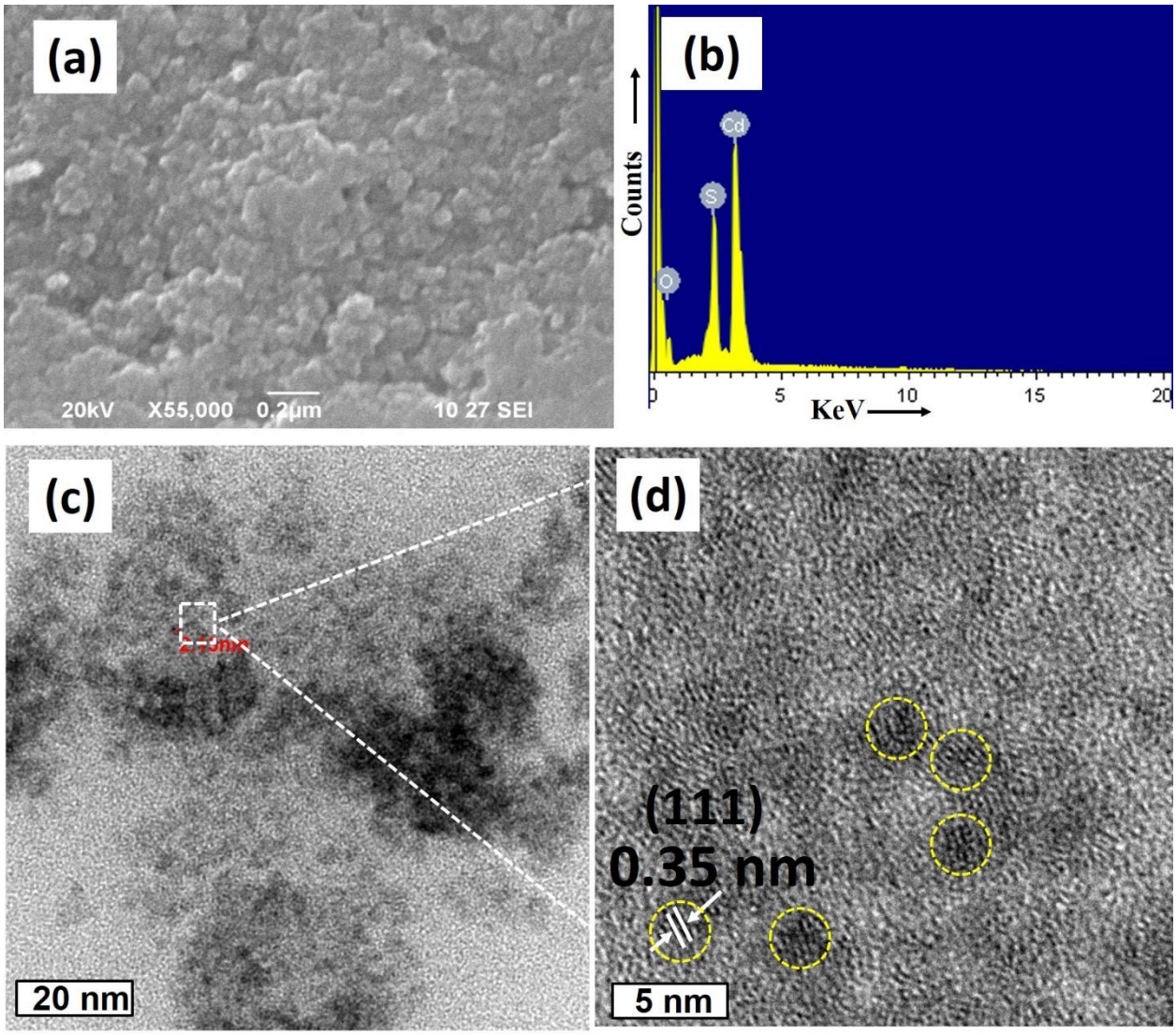

Figure 1. (a) SEM image of CdS QDs; (b) EDAX spectrum of CdS QDs; HR-TEM image of synthesized CdS QDs (c) at 20 nm scale and (d) high magnification at 5 nm scale.

Average particle size estimated from TEM is 3 ±1 nm and thus are considered as quantum dots (<10 nm). In few places QD agglomeration is evident due to the high concentration of

sample loaded on the copper grid for HRTEM analysis.[44] In literature, different QD sizes have been reported (from 4- 10 nm), for instance, 5-10 nm CdS nanoparticles was achieved using *Fusarium* biomass.[45] Borovaya [46] et al. demonstrated *Pleurotus ostreatus* derived CdS QDs of size 4–7 nm. Comparing these reports, the present result of 3-5 nm CdS QDs implies that *Camellia sinensis* extract is highly effective in forming small QDs. In biomass (algae and fungus) based biogenic synthesis, the resultant nanoparticle shape and size distribution is often a challenge and not homogenous. In the case of plant extract based biogenic synthesis, generally, highly stable and homogenous shaped nanoparticles are formed. The high resolution HRTEM image at 5 nm scale (Figure 1d) clearly demonstrates the lattice fringe of CdS QDs. The average lattice diameters between two fringes were found to be 0.33 nm. This implies that the resultant CdS quantum dots belong to (111) cubic crystalline structure of CdS. The existence of (111) crystalline phase was confirmed by X-ray diffraction spectra (**Figure S1** in supporting information). Furthermore, a thin shell layer is observed on the CdS QDs (**Figure S2**, supporting information) which may be attributed to the organic moieties from the tea leaf extract. This is in line with observed oxygen content from EDAX spectra (Figure 1b).

In order to decipher the role of the tea leaf extract in CdS QDs synthesis and observed shell layers on the CdS QDs (**Figure S2**), the FTIR spectra was recorded (See supporting information **Figure S3**). **Figure S3(a)** exhibits multiple absorption peaks that belong to various functional groups presence in the *Camellia sinensis* extract. The peak located around 3441 cm^{-1} can be assigned to the involvement of O-H (alcohol). In the region around 3500 cm^{-1} due to N-H stretching vibration bands of the plant extracts may overlap with the carboxyl band[47]. The significant peak observed at 1649 cm^{-1} (due to stretching of C=O) corresponds to the amide groups (polyphenols, proteins and amino acids). The remaining major peak at 1007 cm^{-1} could be attributed to aliphatic amines.[48] The FTIR features of *Camellia sinensis* extract mediated CdS is presented in **Figure S3 (b)**. Compared to Figure S3 (a), a weak peak observed around

630 cm^{-1} indicates the CdS formation.[49] In addition, significant differences were observed between plant extract (*Camellia sinensis*) and sythesized CdS QDs. Importantly, the peaks appeared at 3421, 1633 and 1376 cm^{-1} corresponding to the O-H (carboxyl group), C=O (amide group: polyphenols, proteins and aminoacids) and N-H bending vibrations of amide-II, respectively imply that the organic residue of *Camellia sinensis* may have immobilized on the surface of CdS nanoparticles. It is anticipated that one of these constituents is involved in the biotransformation based particle size reduction and capping on the CdS QDs.[50] In silver (Ag) nanoparticle synthesis, Sun et al. noticed that polyphenols components from *Camellia sinensis* extract were involved in the reduction of Ag+ ions into Ag nanoparticles[51]. Few other researchers have also experienced a similar type of biotransformation based nanoparticle synthesis [52, 53]. We speculate that proteins binders in the *Camellia sinensis* may play a key role in CdS particle size reduction through amine groups or cysteine residues. A similar observation has been noticed by Rao et al.[43] using *Chlamydomonas reinhardtii* extract based biogenic synthesis. *Chlamydomonas reinhardtii* contains proteins, amino acids and oxidoreductase enzymes, where these enzymes are responsible for biotransformation of CdS nanoparticles.[54, 55] Also, we believe that polyphenols, proteins, caffeine, catechins, theaflavins, thearubigins and aminoacids presence in the *Camellia sinensis* extract may response to the nanosize CdS QDs formation. Based on the above explanation, the plausible mechanism for CdS QDs formation is explained in Scheme 1. While $CdSO_4$ is added to plant extracts, Cd^{2+} ions bind with the plant mediated proteins due to metallic stress. During the addition of Na_2S, it facilitates in the formation of S^{2-} ions that bind to the plant mediated cadmium proteins and results in the synthesis of CdS nanoparticles.

Antibacterial activity of nanoparticles: The antibacterial activity of plant mediated CdS QDs nanoparticles against gram positive (*Streptococcus pyogens* and *Staphylococcus aureus*) and gram negative (*Escherichia coli*, *Serratia marcescens*, *Klebsiella pneumoniae*) bacteria has

been estimated and presented in **Figure 2**. Zone of inhibition was observed for both gram positive and gram negative bacteria. It indicates bactericidal activity of CdS QDs against *Serratia marcescens* followed by *Staphylococcus aureus, Klebsiella pneumoniae*, *Streptococcus pyogens* and *Escherichia coli*. In further analysis, the antibacterial activity found at *Serratia marcescens* implies clear zone and the size of the zone relay on concentrations of CdS QDs (80, 120, 160 and 200 µg/mL). Over all, at higher concentration of CdS QDs 200 µg/mL a clear zone with 21 mm diameter is observed for *Serratia marcescens*. In the case of *K. pneumoniae* and *S. aureus,* the zone diameter is found to be 18 mm and 20 mm diameter respectively. These significant results advocate that the CdS QDs performed as a promising antibacterial agent against both gram positive and negative bacteria. It is noteworthy to mention that the cell wall of the gram positive and gram negative bacteria consists of thick peptidoglycan layer and lipopolysaccharide layer, respectively, which provides strong protection wall from foreign species penetration.[56] Therefore, the observed antibacterial activity of CdS QDs might due to their low-dimension particle size (3-5 nm), which is able to penetrate and pass through the nanopores of the bacteria cell wall thus enhancing the broad spectrum of antibacterial activity against the virulent bacteria.

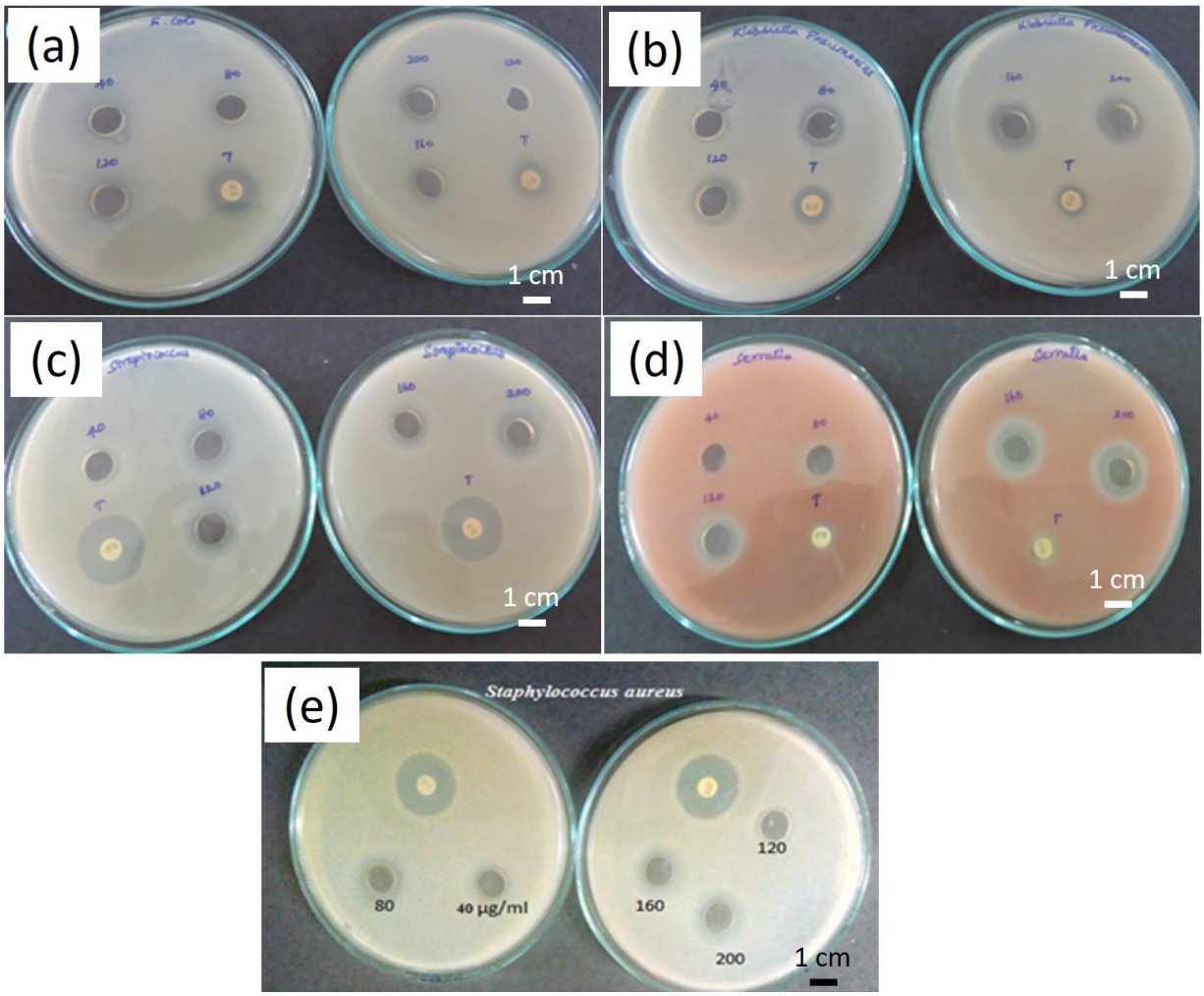

Figure 2. CdS QDs against (a) *Escherichia coli* (b) *Klebsiellapneumoniae* (c) *Streptococcus pyogens* (d) *Serratiamarcescens* and (e) *Staphylococcus aureus* [Note: ampicillin (10µg) and streptomycin (10µg) were used as control in each measurement].

Hemolysis activity: Hemolysis of the blood is a major issue associated with foreign materials like implants while inserted in the human body.[57] The red blood cells (RBC) will be hemolysed when in contact with water. Therefore, biocompatibility of plant extract derived CdS QDs is studied through investigating hemolytic activity in RBC cells.

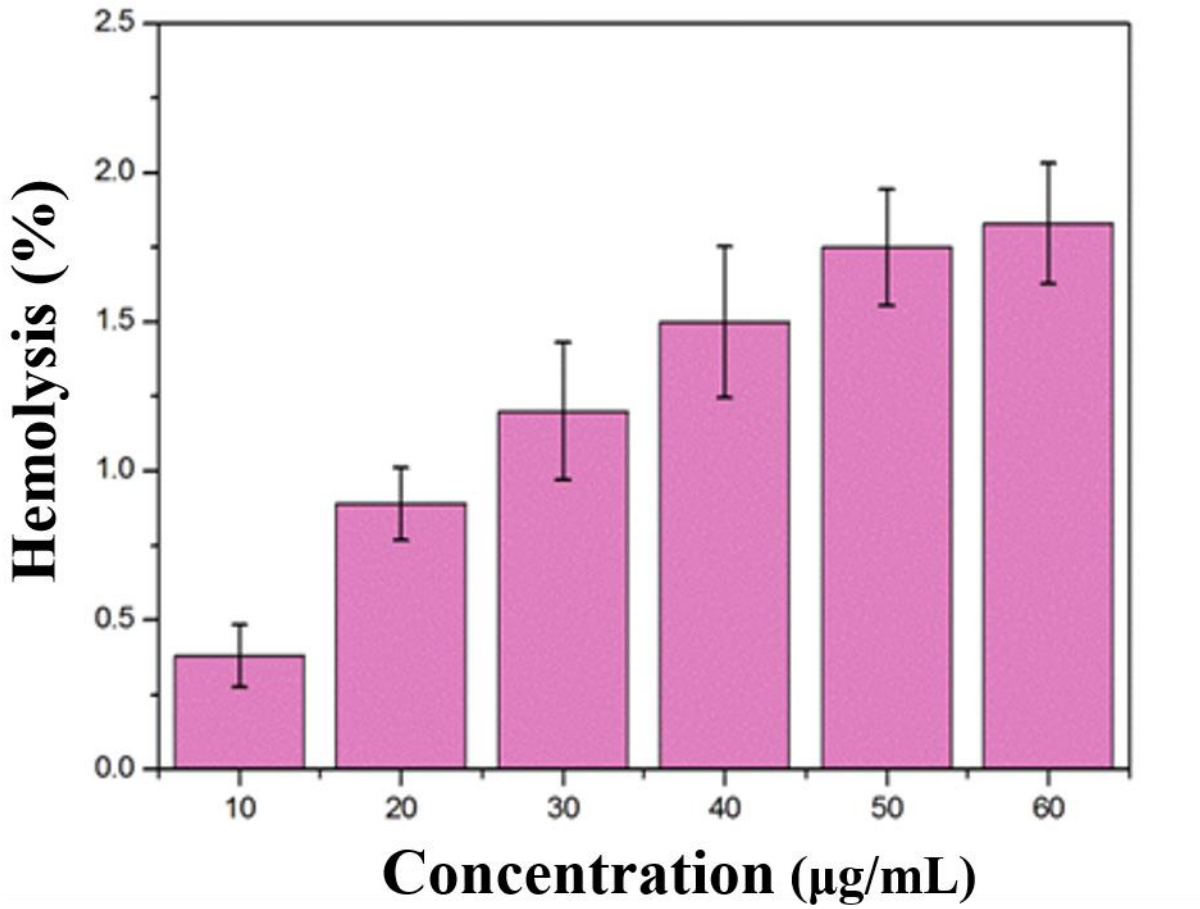

Figure 3. The hemolysis activity for different concentration CdS QDs [note: measurements recorded after 3 hours by UV spectrophotometer at 541 nm].

For this analysis, the water was added to the RBC cells and then the released haemoglobin was measured using optical spectrophotometer (100% hemolysis). The estimated percentage of hemolytic activity of RBC at various CdS QD concentrations is summarised in **Figure 3**. From **Figure 3**, it seems that the hemolysis rate of CdS QDs in RBC monotonically increased and relay on dose concentration. At higher concentration of 60 µg/mL, the hemolysis rate is found to be 1.83 ±0.20%. Singhal *et al.*[58] suggested that foreign biomaterial exhibits below 5% hemolysis, which is permissible in therapeutic /biomedical applications. For more understanding, the optical images of RBC cells in associate with higher concentration of CdS QDs at 60 µg/mL is

as shown in **Figure S4** (see supporting information) compared with control (in the absence of QDs). It further endorses that *Camellia sinensis* derived CdS QDs does not produce significant morphological changes in RBC cells compared to untreated cell (in the absence of QDs).

Cytotoxicity analysis: cytotoxic effect of the synthesized CdS QDs, against A549 cell line was studied. MTT assay was used to assess the effect of CdS QDs on proliferation of A549 cell line. The percentage of cell viability for different CdS QDs concentrations were examined at 24 h and compared with standard drug cisplatin (**Figure 4**). **Figure 4** implies that inhibition of A549 cells are gradually increased with CdS QDs concentration and is comparable with standard drug cisplatin (14 µg/mL) in 24 h period.

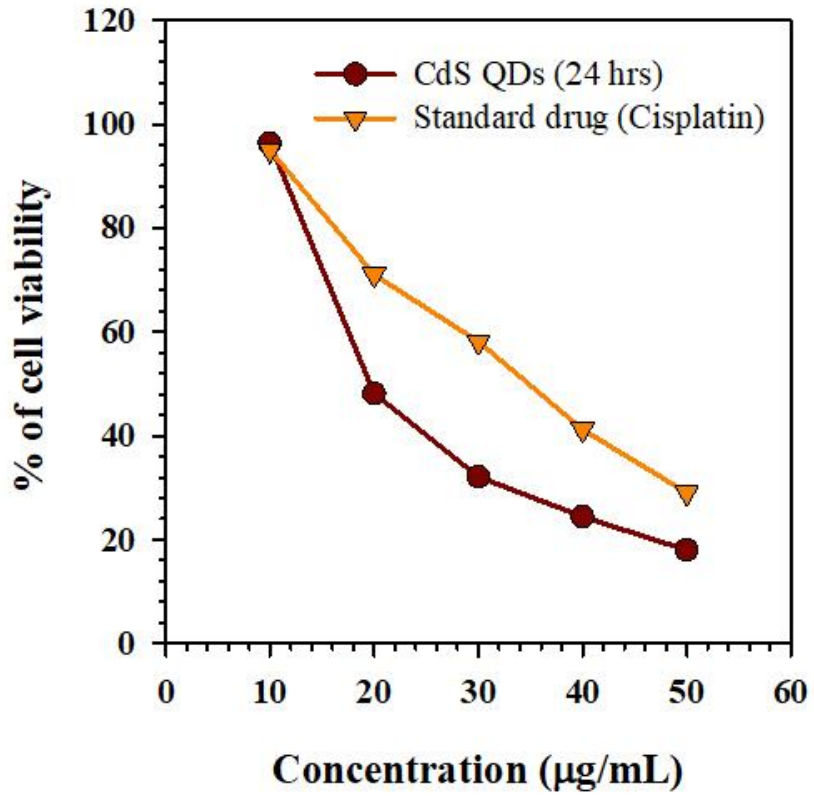

Figure 4. Cytotoxicity effect of A549 cell line treated with green CdS QDs and standard drug cisplatin.

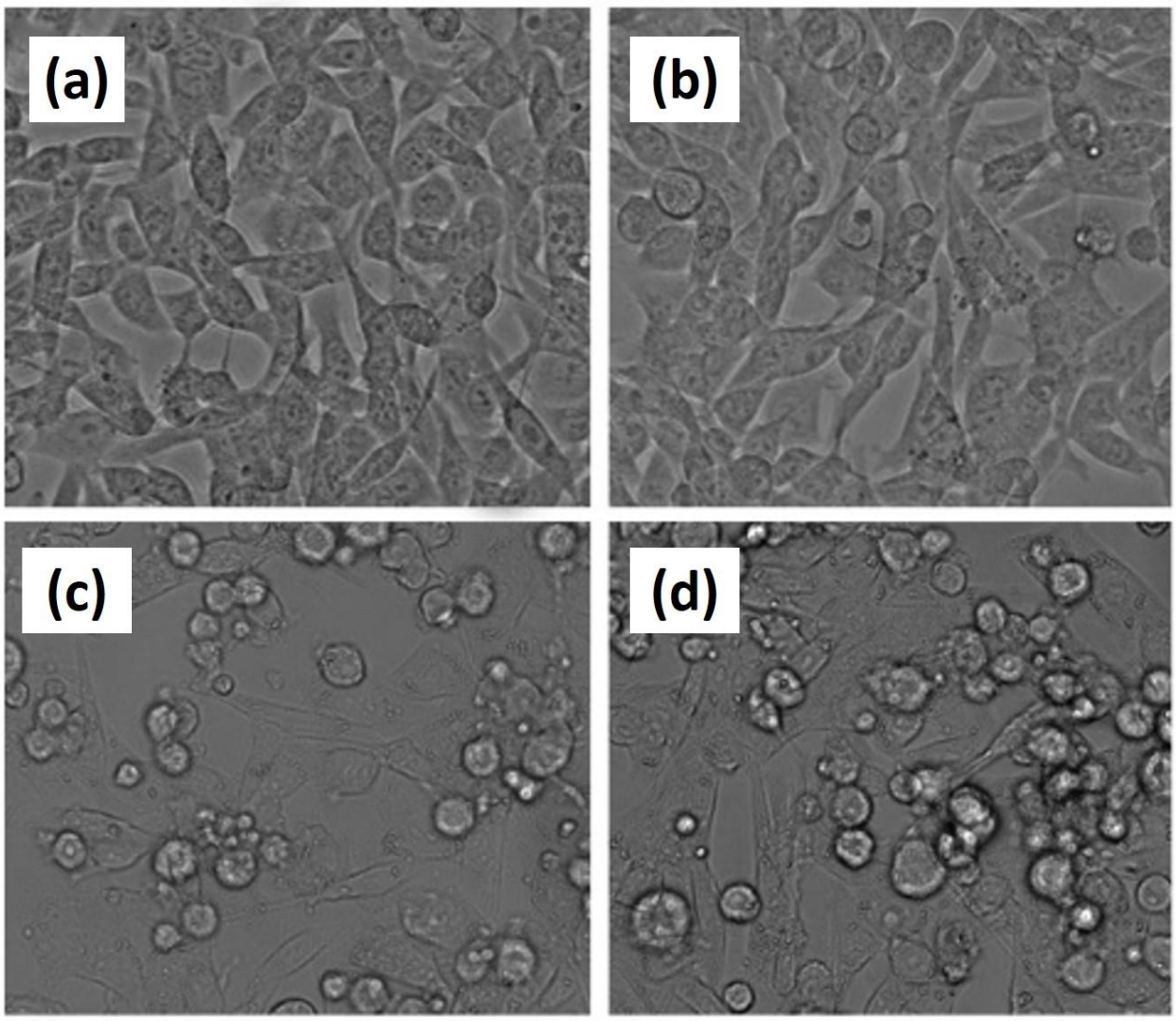

Figure.5 Optical microscope images of cytotoxicity effect observed at A549 cell line (a) control [untreated]; and treated with CdS QDs (b) 10 µg/mL, (c) 25 µg/mL and (d) 50 µg/mL [noted that images of A549 cell line is recorded after 24 hours].

The enhanced cytotoxic effect by CdS may ascribe to chemical interaction between CdS and A549 cell bio-environment. Furthermore, to ensure the CdS QDs/ bio-environment interface, the phase contrast microscope images were recorded and are presented in **Figure 5 (a) – (d)**. Compared to an untreated cell (**Figure 5a**), the CdS QDs treated cells (**Figure 5b, 5c** and **5d**) showed significant morphological changes due to A549 cell shrinkage, loss of membrane

integrity, cytoplasmic condensation and also cell growth inhibition.[59] The plausible reason for the degradation of the A549 cells might be due to chemical interaction between CdS QDs and A549 cell. Briefly, green synthesized CdS QDs particles could interact with the phosphorous moieties in DNA. Then DNA replication is inactivated leading to inhibition of enzyme functions which results in loss of cell viability, further it undergoes cell death through apoptosis.

Fluorescence imaging analysis: The observed apoptosis effect from **Figure 5** raise the question on which cycle of A549 cells growth is inhibited by CdS QDs. Therefore, we examine the apoptotic cell inhibition at different stages using fluorescence imaging.

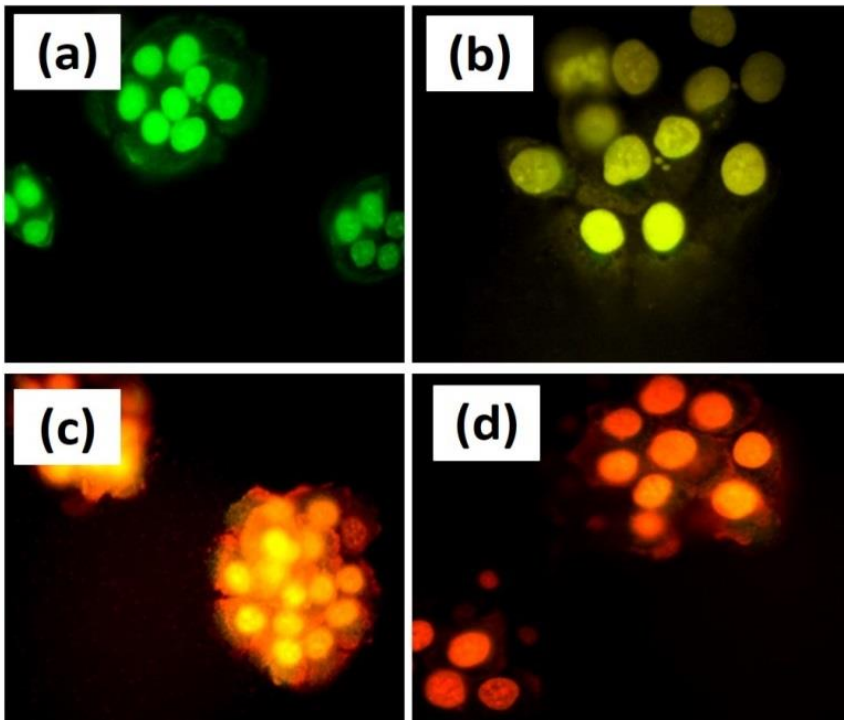

Figure 6. Fluorescence microscopy images of AO/EtBr stained A549 cells (a) untreated (control) and; CdS QDs treated at different concentration (b) 10, (c) 25 and (d) 50 µg/mL. Note that AO/EtBr images are recorded using laser light excitation at 460 nm.

Due to the fact that fluorescence imaging uses different dyes it may not precisely portrait the cell condition. For instance, the acridine orange (AO) is a promising dye material it can bind both viable and dead cells. But in the case of ethidium bromide (EtBr), it only binds with dead cells due to loss of membrane integrity. When both AO/EtBr staining used in CdS QDs treated A549 cells we can qualitatively distinguish the influence of CdS QDs. **Figure 6 (b-d)** illustrates CdS QDs treated A549 cells at different concentration 10, 25 and 50 µg/mL after 24 h of incubation. The untreated A549 cells (**Figure 6a**) showing green colour implies live cells. In the case of **Figure 6b-d** shows different colours such as yellow (24 µg/mL), red (48 µg/mL), and orange (96 µg/mL), corresponding to early apoptotic cells, necrotic cells and late apoptotic cells, respectively. Based on this analysis, it is understood that the apoptosis effect at A549 cells is dependent on the CdS QDs concentration. The influence of CdS QDs on A549 cells occurred for several reasons including a) changes in chromatin condensation, b) fragmented nuclei and c) membrane blebbing.[60] These factors were verified using another dye, DAPI, through a DAPI stain test (See supporting information **Figure S6**).

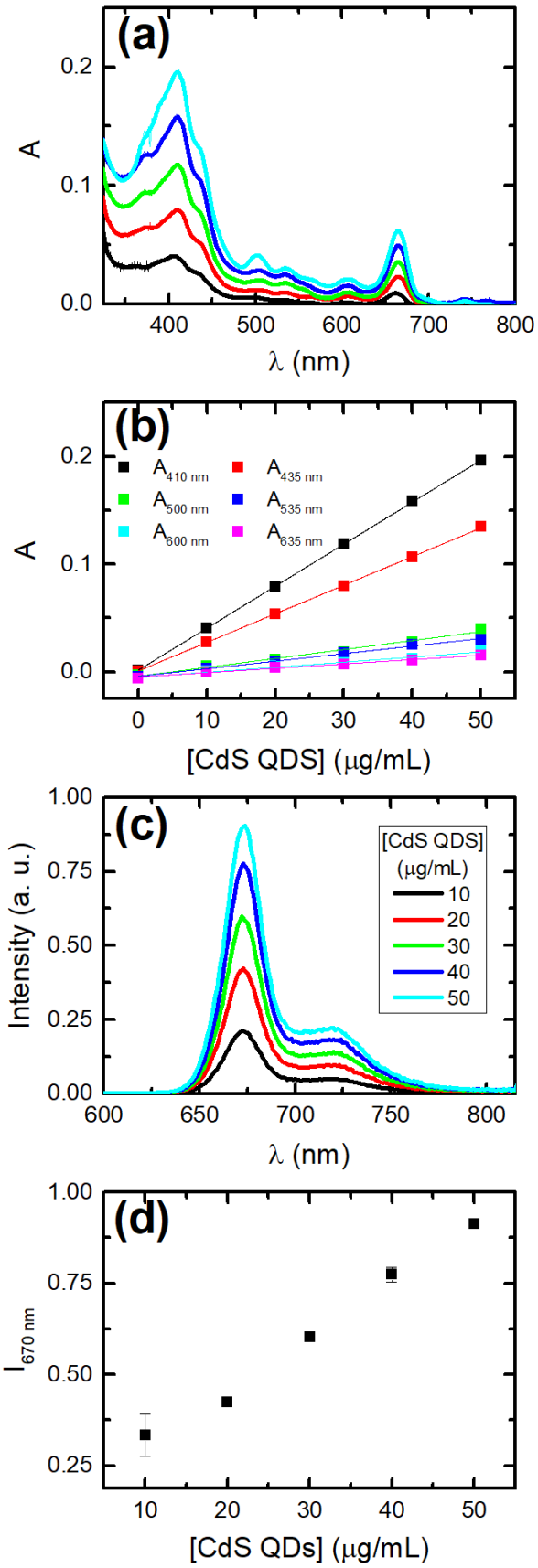

Figure 7. (a) Absorption and (b) fluorescence emission spectra (λexc= 410 nm) of Camellia sinensis derived Green CdS Quantum Dots in ethanol at different concentrations at room

temperature. (c) Absorbance at 410, 435, 500, 535, 600 and 635 nm and (d) fluorescence emission intensity at 670 nm as a function of the concentration. Absorbance spectra were smoothed (thick line) using the Savitzky-Golay method (22 points) but original are also plotted (thin line).

It is noteworthy to discuss the unprecedented intracellular fluorescence images of the CdS QD treated A549 cells. Though these CdS QDs are not covered with any additional shell layer (ZnS, CdTe) they show high brightness and contrast images compared to recent articles on A549 cell tracking.[61] Further analysis of the fluorescence properties of *Camellia sinensis* derived CdS QDs could explain why these CdS QDs produce effective intracellular fluorescence intensity. The absorption and fluorescence spectra of CdS QDs are presented in **Figure 7 (a) - (d),** respectively.

Figure 7 (a) shows the optical absorption spectra recorded at different wavelength. The strong optical absorbance peak observed around ~410-420 nm indicates the band edge of CdS QDs. Further recording optical absorbance quantity at different monochromatic wavelength (**Figure 7 (b)**) is clearly infers that CdS QDs have high optical absorbance at 410 nm. This is corresponding to 3.03 eV band gap energy. This implies that *Camellia sinensis* derived CdS QDs result ~0.53 eV higher than that of bulk CdS band gap energy (~2.4 eV) due to quantum confinement effect.[62-63] The optical absorbance of CdS QDs increases with QD concentration (**Figure 7c**). From **Figure 7 (d)**, the observed fluorescence emission ~670 nm is gradually enhanced with CdS QDs concentration. This enhanced fluorescence emission is responsible for the high contrast fluorescence bioimaging results obtained at **Figure 6 (b)-(c)**.

Cell cycle analysis: Optical (Figure 5) and florescence microscopy (figure 6) demonstrate A549 cell death with CdS QDs treatment, thus the underlying mechanism of CdS QDs in arresting the cell cycle of A549 cells should be understood. In this view, the fluorescence-activated cell

sorting (FACS) analysis is a promising technique to exclusively evaluate the DNA content in different phases such as Go/G1, S and G2/M. During the G_1 phase, DNA content within the cell. In S phase DNA replication will takes place and G_2/M phase cells are divided into two daughter cells. The representative images of DNA flow cytometry is presented in **Figure 8**.

Figure 8 (a-d) depicts the DNA count in untreated and CdS QDs treated A549 cells measured at 24 h incubation. The cell death rate results can be easily accounted from **Figure 8**. Comparing the DNA count in Go/G1, S and G2/M phases, S phase showed striking A549 cells death rate. The quantitative results are summarised in **Figure S6**. For S phase, the DNA count in untreated A549 cell was of 31.78% and gradually diminished to 14.98 under CdS QDs treatment (50 µg/mL). The similar DNA count degradation tendency is observed in G2M phase. This apoptosis effect is the reason for noticing A549 cell death in **Figure 5(c-d)** which clearly explains the key role of CdS QDs interaction with A549 cell.

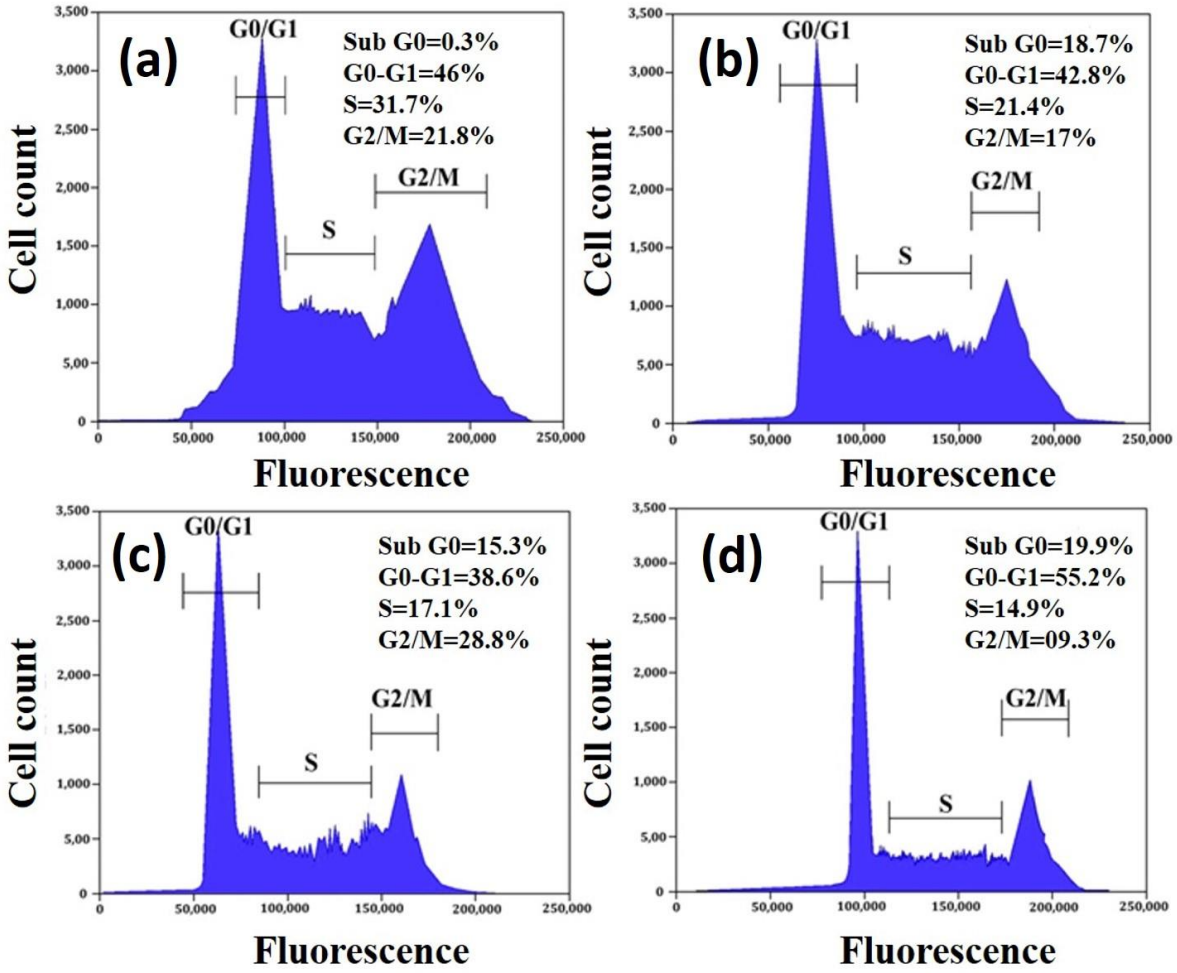

Figure 8. DNA flow cytometry of A549 cells recorded at 24 h incubation (a) control (untreated); and treated with CdS QDs (b) 10, (c) 25 and (d) 50 µg/mL.

Furthermore, it is cross verified that the apoptosis effect occurred at the S stage, through flow cytometry using Annexin – FITC/ PI dual fluorescence staining. The representative flow cytometry Annexin – FITC/ PI dual fluorescence images is presented in **Figure 9 (a-d)**. The early apoptotic cells will bind with Annexin. In the case of dead and late apoptotic cells are binds with both Annexin – FTIC and PI staining.[64] The percentage of apoptotic cells is higher at CdS QDs treated A549 cells compared to untreated cells **(Figure 9a)**. The estimated cells from **Figure 9 (a-d)** are compared in **Figure S7**. The overall results explain that early and late apoptotic cells are CdS QDs dose dependence increased from 28.05, 51.85 and 77.0% compared to control cells. As is explained earlier, the cell cycle arrest might be induced by

green synthesized CdS QDs, that have entered into the nucleus wall through the pores and interacting with the DNA. [65]

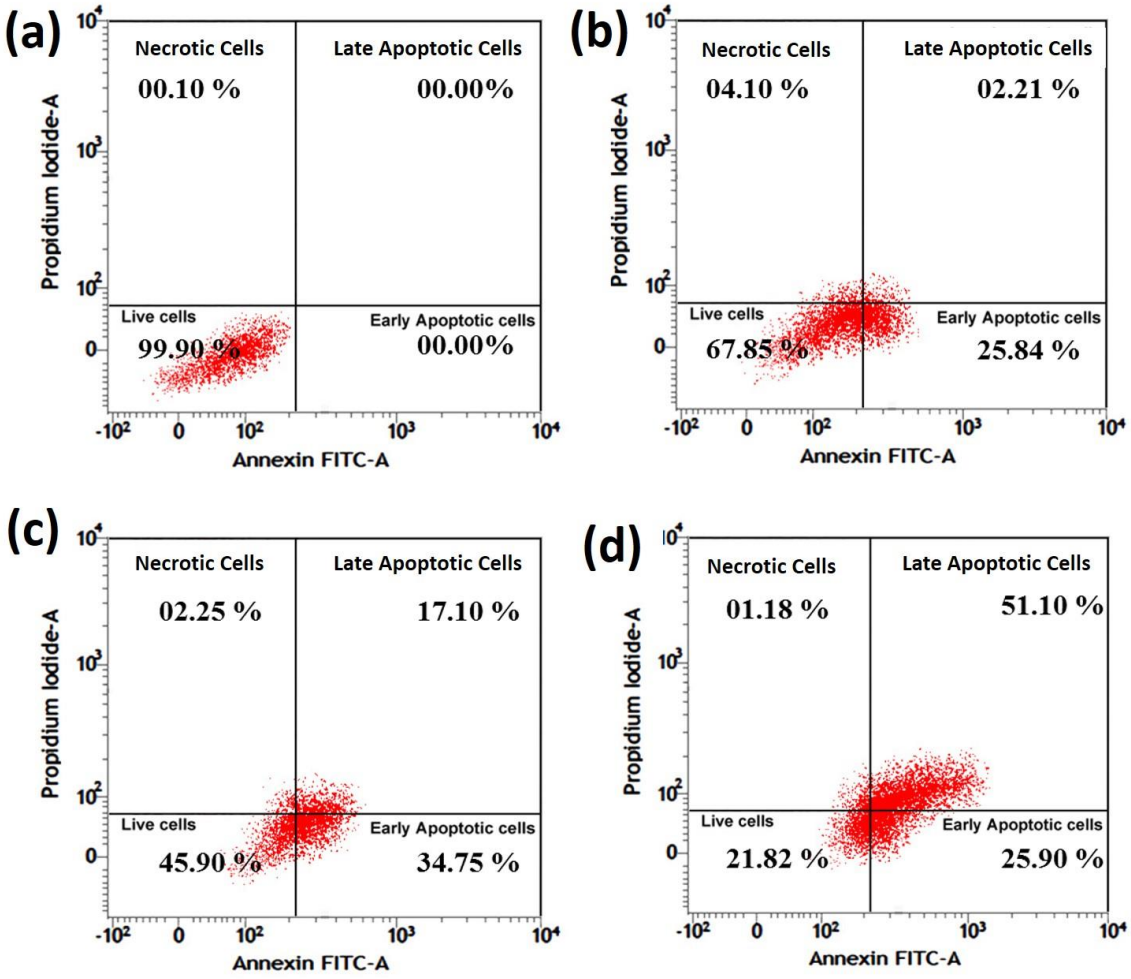

Figure 9. The apoptotic cell death in A549 cells analysed by flow cytometry using Annexin – FITC/PI staining (a) control (untreated) and; CdS QDs (b) 10 (c) 25 and (d) 50 µg/mL. Note that the fluorescence intensity of Annexin – FITC/PI stained apoptotic cells expressed at the top and bottom right quadrants are in late and early apoptosis, respectively.

As **Figure 8** illustrates, DNA count ratio of A549 cells degraded in S and G2M phase, the major effect of apoptosis occurred in S phase and is undoubtedly explained in **Figure 9**. Therefore, we can conclude that plant extract mediated CdS QDs induced cell cycle arrest and has occurred at S phase. The effective bioimaging and apoptosis effect exists at CdS QDs

treated A549 cells strongly advocate that *Camellia sinensis* extract mediated QDs are futuristic in simultaneous bioimaging and therapeutic applications. In particular, examining these CdS QDs at *in vivo* condition will facilitate the cytotoxic effect in real-time bio-environment. Surprisingly, these green CdS QDs treated with healthy RBC cells do not show any morphological changes. These results endorse the biocompatibility nature of CdS QDs and encourage further *in-vivo* applications. Recent reviews state that cytotoxicity of Cd based QDs are less at *in vivo* condition compared to *in vitro*.[66-68] Because, heavy-metal release and generation of reactive oxygen species will enhance the cytotoxicity at *in vitro*. In this condition, QDs may interact directly with blood components. In addition, QDs formulation is differ with synthesis protocol, size, surface chemistry.[69] Therefore, a careful *in vivo* examination will be helpful in further standardising these green CdS QDs in cancer cell imaging and treatment. From a materials point of view, the influence of plant extract concentration on CdS particle size through surface passivation with appropriate biomolecules[43, 70] will also promote this QDs in wide range of biological activity based applications.

Conclusions

In this work, for the first time, biological activity of *Camellia sinensis* extract mediated CdS quantum dots is demonstrated. The organic moieties such as polyphenol and protiens presence in the plant extract play a key role in stabilizing highly homogeneous CdS spherical nanoparticles ranging from 3 to 5 nm. Owing to the high florescence emission and quantum confinement effect results green CdS QDs are producing effective intracellular fluorescence cell tracking at A549 lung cancer cell. Furthermore, these low dimensional CdS QDs penetrate into nanopores of A549 cells and degrade the cell (cell death). The flow cytometry results confirm that *Camellia sinensis* extract mediated CdS quantum dots are highly reactive and stable in bioenvironment. The flow cytometry analysis confirms that CdS QDs arrested S phase of A549 cells. The experimental results suggest the *Camellia sinensis* extract mediated CdS

QDs are promising low dimensional biomaterial for wide range of biomedical applications (antibacterial, bioimaging and therapeutic). Interestingly, the *Camellia sinensis* extract will be obtained from not only fresh leaves, also mother leaves can be used which reduce the overall synthesis cost compare to conventional chemical stabilizers. Further investigating the influence of *Camellia sinensis* extract concentration on CdS QDs size, CdS QDs/cell interfaces will be further interest for transforming green CdS QDs towards *in vivo* based applications.

ASSOCIATED CONTENT

The following files are available free of charge. Details of FTIR, hemolysis assay results, antibacterial activity, DAPI images, flow cytometer results.

AUTHOR INFORMATION

Corresponding Author

* mythumithras@gmail.com (BMG); S.pitchaimuthu@swansea.ac.uk (SP).

ACKNOWLEDGMENT

The authors grateful thank the Principal and Head, Department of Biotechnology, K.S.Rangasammy College of Technology, Tiruchengode, Tamil Nadu, India for the support offered towards study. The authors also acknowledge DST-FIST (fund for infrastructure) for science and technology (SR/FST/College-235/2014 dated 21.11.2014). We also thank to Kanan Devan Hills plantations company (p) ltd, Munnar, Kerala, for their constant support. S.P. acknowledges Welsh Government and European Regional Development Fund for supporting Rising Star Fellowship (80761-SU-102 (West)). MLD and CDC are grateful for the financial support of the EPSRC and Innovate UK for the SPECIFIC Innovation and Knowledge Centre (grant numbers EP/I019278/1, EP/K000292/1, EP/L010372/1) and the European

Regional Development Fund through the Welsh Government for support to the Sêr Solar program.

ABBREVIATIONS

CdS QDs, cadmium sulfide quantum dots; ROS, reactive oxygen species; RBC, red blood cells; HrTEM, high resolution transmission electron microscopy; DNA, Deoxyribonucleic acid; PI, propidium iodide.

REFERENCES

1. Erten, A.; Hall, D. J.; Hoh, C. K.; Cao, H. S. T.; Kaushal, S.; Esener, S. C.; Hoffman, R. M.; Bouvet, M.; Chen, J.; Kesari, S.; Makale, M. T. In *Enhancing magnetic resonance imaging tumor detection with fluorescence intensity and lifetime imaging*, SPIE: 2010; p 6.
2. Frasco, M. F.; Chaniotakis, N., Bioconjugated quantum dots as fluorescent probes for bioanalytical applications. *Analytical and Bioanalytical Chemistry* **2010,** *396*, 229-240.
3. Bagalkot, V.; Zhang, L.; Levy-Nissenbaum, E.; Jon, S.; Kantoff, P. W.; Langer, R.; Farokhzad, O. C., Quantum Dot−Aptamer Conjugates for Synchronous Cancer Imaging, Therapy, and Sensing of Drug Delivery Based on Bi-Fluorescence Resonance Energy Transfer. *Nano letters* **2007,** *7* , 3065-3070.
4. Jain, K., Advances in the field of nanooncology. *BMC Medicine* **2010,** *8*, 83.
5. Ciesielska, E.; Gwardys, A.; Metodiewa, D., Anticancer, antiradical and antioxidative actions of novel Antoksyd S and its major components, baicalin and baicalein. *Anticancer Res* **2002,** *22*, 2885-2891.
6. Li-Weber, M., New therapeutic aspects of flavones: the anticancer properties of Scutellaria and its main active constituents Wogonin, Baicalein and Baicalin. *Cancer treatment reviews* **2009,** *35*, 57-68.
7. Kim, D. K.; Dobson, J., Nanomedicine for targeted drug delivery. *Journal of Materials Chemistry* **2009,** *19*, 6294-6307.
8. Vikas, J.; Shikha, J.; Mahajan, S. C., Nanomedicines Based Drug Delivery Systems for Anti-Cancer Targeting and Treatment. *Current Drug Delivery* **2015,** *12*, 177-191.
9. Khan, M. I.; Mohammad, A.; Patil, G.; Naqvi, S. A.; Chauhan, L. K.; Ahmad, I., Induction of ROS, mitochondrial damage and autophagy in lung epithelial cancer cells by iron oxide nanoparticles. *Biomaterials* **2012,** *33*, 1477-88.
10. Chen, N.; He, Y.; Su, Y.; Li, X.; Huang, Q.; Wang, H.; Zhang, X.; Tai, R.; Fan, C., The cytotoxicity of cadmium-based quantum dots. *Biomaterials* **2012,** *33*, 1238-44.
11. Wu, Y. N.; Yang, L. X.; Shi, X. Y.; Li, I. C.; Biazik, J. M.; Ratinac, K. R.; Chen, D. H.; Thordarson, P.; Shieh, D. B.; Braet, F., The selective growth inhibition of oral cancer by iron core-gold shell nanoparticles through mitochondria-mediated autophagy. *Biomaterials* **2011,** *32* , 4565-73.
12. Ahamed, M.; Akhtar, M. J.; Raja, M.; Ahmad, I.; Siddiqui, M. K.; AlSalhi, M. S.; Alrokayan, S. A., ZnO nanorod-induced apoptosis in human alveolar adenocarcinoma cells via p53, survivin and bax/bcl-2 pathways: role of oxidative stress. *Nanomedicine : nanotechnology, biology, and medicine* **2011,** *7*, 904-13.
13. Li, K. G.; Chen, J. T.; Bai, S. S.; Wen, X.; Song, S. Y.; Yu, Q.; Li, J.; Wang, Y. Q., Intracellular oxidative stress and cadmium ions release induce cytotoxicity of unmodified cadmium sulfide quantum dots. *Toxicology in vitro : an international journal published in association with BIBRA* **2009,** *23*, 1007-13.

14. Liu, W.; Zhang, S.; Wang, L.; Qu, C.; Zhang, C.; Hong, L.; Yuan, L.; Huang, Z.; Wang, Z.; Liu, S.; Jiang, G., CdSe Quantum Dot (QD)-Induced Morphological and Functional Impairments to Liver in Mice. *PLoS ONE* **2011,** *6* , e24406.
15. Zheng, X. T.; Ananthanarayanan, A.; Luo, K. Q.; Chen, P., Glowing graphene quantum dots and carbon dots: properties, syntheses, and biological applications. *Small (Weinheim an der Bergstrasse, Germany)* **2015,** *11* , 1620-36.
16. Li, L.; Wu, G.; Yang, G.; Peng, J.; Zhao, J.; Zhu, J. J., Focusing on luminescent graphene quantum dots: current status and future perspectives. *Nanoscale* **2013,** *5*, 4015-39.
17. Zhang, M.; Bai, L.; Shang, W.; Xie, W.; Ma, H.; Fu, Y.; Fang, D.; Sun, H.; Fan, L.; Han, M.; Liu, C.; Yang, S., Facile synthesis of water-soluble, highly fluorescent graphene quantum dots as a robust biological label for stem cells. *Journal of Materials Chemistry* **2012,** *22*, 7461-7467.
18. Jiang, D.; Chen, Y.; Li, N.; Li, W.; Wang, Z.; Zhu, J.; Zhang, H.; Liu, B.; Xu, S., Synthesis of Luminescent Graphene Quantum Dots with High Quantum Yield and Their Toxicity Study. *PLOS ONE* **2016,** *10*, e0144906.
19. Zhou, X.; Zhang, Y.; Wang, C.; Wu, X.; Yang, Y.; Zheng, B.; Wu, H.; Guo, S.; Zhang, J., Photo-Fenton reaction of graphene oxide: a new strategy to prepare graphene quantum dots for DNA cleavage. *ACS nano* **2012,** *6* , 6592-9.
20. Pan, D.; Zhang, J.; Li, Z.; Wu, M., Hydrothermal route for cutting graphene sheets into blue-luminescent graphene quantum dots. *Advanced materials (Deerfield Beach, Fla.)* **2010,** *22* , 734-8.
21. Martynenko, I. V.; Litvin, A. P.; Purcell-Milton, F.; Baranov, A. V.; Fedorov, A. V.; Gun'ko, Y. K., Application of semiconductor quantum dots in bioimaging and biosensing. *Journal of Materials Chemistry B* **2017,** *5*, 6701-6727.
22. Onoshima, D.; Yukawa, H.; Baba, Y., Multifunctional quantum dots-based cancer diagnostics and stem cell therapeutics for regenerative medicine. *Advanced Drug Delivery Reviews* **2015,** *95*, 2-14.
23. Singh, B. R.; Singh, B. N.; Khan, W.; Singh, H. B.; Naqvi, A. H., ROS-mediated apoptotic cell death in prostate cancer LNCaP cells induced by biosurfactant stabilized CdS quantum dots. *Biomaterials* **2012,** *33*, 5753-5767.
24. Lakshmipathy, R.; Sarada, N. C.; Chidambaram, K.; Pasha, S. K., One-step, low-temperature fabrication of CdS quantum dots by watermelon rind: a green approach. *International Journal of Nanomedicine* **2015,** *10* , 183-188.
25. Jacob, J. M.; Lens, P. N. L.; Balakrishnan, R. M., Microbial synthesis of chalcogenide semiconductor nanoparticles: a review. *Microbial Biotechnology* **2016,** *9* , 11-21.
26. Zhang, X.; Yan, S.; Tyagi, R. D.; Surampalli, R. Y., Synthesis of nanoparticles by microorganisms and their application in enhancing microbiological reaction rates. *Chemosphere* **2011,** *82*, 489-94.
27. Reddy, A. S.; Chen, C.-Y.; Baker, S. C.; Chen, C.-C.; Jean, J.-S.; Fan, C.-W.; Chen, H.-R.; Wang, J.-C., Synthesis of silver nanoparticles using surfactin: A biosurfactant as stabilizing agent. *Materials Letters* **2009,** *63*, 1227-1230.
28. Di Benedetto, F.; Camposeo, A.; Persano, L.; Laera, A. M.; Piscopiello, E.; Cingolani, R.; Tapfer, L.; Pisignano, D., Light-emitting nanocomposite CdS-polymer electrospun fibres via in situ nanoparticle generation. *Nanoscale* **2011,** *3*, 4234-4239.
29. Singh, B. R.; Dwivedi, S.; Al-Khedhairy, A. A.; Musarrat, J., Synthesis of stable cadmium sulfide nanoparticles using surfactin produced by Bacillus amyloliquifaciens strain KSU-109. *Colloids and surfaces. B, Biointerfaces* **2011,** *85*, 207-13.
30. Zou, Y.; Li, D.; Yang, D., Shape and phase control of CdS nanocrystals using cationic surfactant in noninjection synthesis. *Nanoscale Research Letters* **2011,** *6*, 374.

31. Borovaya, M. N.; Naumenko, A. P.; Matvieieva, N. A.; Blume, Y. B.; Yemets, A. I., Biosynthesis of luminescent CdS quantum dots using plant hairy root culture. *Nanoscale Research Letters* **2014,** *9*, 686.
32. Kalishwaralal, K.; Deepak, V.; Ram Kumar Pandian, S.; Gurunathan, S., Biological synthesis of gold nanocubes from Bacillus licheniformis. *Bioresource technology* **2009,** *100*, 5356-5358.
33. Li, H.; Shih, W. Y.; Shih, W.-H., Synthesis and Characterization of Aqueous Carboxyl-Capped CdS Quantum Dots for Bioapplications. *Industrial & Engineering Chemistry Research* **2007,** *46*, 2013-2019.
34. Galeone, A.; Vecchio, G.; Malvindi, M. A.; Brunetti, V.; Cingolani, R.; Pompa, P. P., In vivo assessment of CdSe-ZnS quantum dots: coating dependent bioaccumulation and genotoxicity. *Nanoscale* **2012,** *4*, 6401-6407.
35. Ahmad, A.; Mukherjee, P.; Mandal, D.; Senapati, S.; Khan, M. I.; Kumar, R.; Sastry, M., Enzyme Mediated Extracellular Synthesis of CdS Nanoparticles by the Fungus, Fusarium oxysporum. *Journal of the American Chemical Society* **2002,** *124*, 12108-12109.
36. Prasad, K.; Jha, A. K., Biosynthesis of CdS nanoparticles: An improved green and rapid procedure. *Journal of Colloid and Interface Science* **2010,** *342*, 68-72.
37. Qi, P.; Zhang, D.; Zeng, Y.; Wan, Y., Biosynthesis of CdS nanoparticles: A fluorescent sensor for sulfate-reducing bacteria detection. *Talanta* **2016,** *147*, 142-146.
38. Malarkodi, C.; Rajeshkumar, S.; Paulkumar, K.; Vanaja, M.; Gnanajobitha, G.; Annadurai, G., Biosynthesis and Antimicrobial Activity of Semiconductor Nanoparticles against Oral Pathogens. *Bioinorganic Chemistry and Applications* **2014,** *2014*, 11.
39. Prasad, K. S.; Amin, T.; Katuva, S.; Kumari, M.; Selvaraj, K., Synthesis of water soluble CdS nanoparticles and study of their DNA damage activity. *Arabian Journal of Chemistry* **2017,** *10*, S3929-S3935.
40. Shanthi, K.; Vimala, K.; Gopi, D.; Kannan, S., Fabrication of a pH responsive DOX conjugated PEGylated palladium nanoparticle mediated drug delivery system: an in vitro and in vivo evaluation. *RSC Advances* **2015,** *5* , 44998-45014.
41. Vivek, R.; Ramar, T.; Muthuchelian, K.; Gunasekaran, P.; Kaveri, K.; Kannan, S., *Green biosynthesis of silver nanoparticles from Annona squamosa leaf extract and its in vitro cytotoxic effect on MCF-7 cells*. **2012**, 47, 2405-2410.
42. Vivek, R.; Thangam, R.; Muthuchelian, K.; Gunasekaran, P.; Kaveri, K.; Kannan, S., Green biosynthesis of silver nanoparticles from Annona squamosa leaf extract and its in vitro cytotoxic effect on MCF-7 cells. *Process Biochemistry* **2012,** *47*, 2405-2410.
43. Rao, M. D.; Pennathur, G., Green synthesis and characterization of cadmium sulphide nanoparticles from Chlamydomonas reinhardtii and their application as photocatalysts. *Materials Research Bulletin* **2017,** *85,* 64-73.
44. Jiang, J.; Oberdörster, G.; Biswas, P., Characterization of size, surface charge, and agglomeration state of nanoparticle dispersions for toxicological studies. *Journal of Nanoparticle Research* **2009,** *11*, 77-89.
45. Ahmad, A.; Mukherjee, P.; Mandal, D.; Senapati, S.; Khan, M.; Kumar, R.; Sastr, M., Enzyme-mediated extracellular synthesis of CdS nanoparticles by the fungus, Fusarium oxysporum. *J Am Chem Soc* **2002,** *124*.
46. Borovaya, M.; Pirko, Y.; Krupodorova, T.; Naumenko, A.; Blume, Y.; Yemets, A., Biosynthesis of cadmium sulphide quantum dots by using Pleurotus ostreatus (Jacq.) P. Kumm. *Biotechnology & Biotechnological Equipment* **2015,** *29*, 1156-1163.
47. Choi, S. B.; Yun, Y. S., Biosorption of cadmium by various types of dried sludge: an equilibrium study and investigation of mechanisms. *J Hazard Mater* **2006,** *138*, 378-83.

48. Chen, G.; Yi, B.; Zeng, G.; Niu, Q.; Yan, M.; Chen, A.; Du, J.; Huang, J.; Zhang, Q., Facile green extracellular biosynthesis of CdS quantum dots by white rot fungus Phanerochaete chrysosporium. *Colloids and surfaces. B, Biointerfaces* **2014,** *117*, 199-205.
49. Murugadoss, G.; Thangamuthu, R.; Jayavel, R.; Rajesh Kumar, M., Narrow with tunable optical band gap of CdS based core shell nanoparticles: Applications in pollutant degradation and solar cells. *Journal of Luminescence* **2015,** *165*, 30-39.
50. Chen, C.; Peng, J.; Xia, H.-S.; Yang, G.-F.; Wu, Q.-S.; Chen, L.-D.; Zeng, L.-B.; Zhang, Z.-L.; Pang, D.-W.; Li, Y., Quantum dots-based immunofluorescence technology for the quantitative determination of HER2 expression in breast cancer. *Biomaterials* **2009,** *30*, 2912-2918.
51. Sun, Q.; Cai, X.; Li, J.; Zheng, M.; Chen, Z.; Yu, C.-P., Green synthesis of silver nanoparticles using tea leaf extract and evaluation of their stability and antibacterial activity. *Colloids and Surfaces A: Physicochemical and Engineering Aspects* **2014,** *444*, 226-231.
52. Begum, N. A.; Mondal, S.; Basu, S.; Laskar, R. A.; Mandal, D., Biogenic synthesis of Au and Ag nanoparticles using aqueous solutions of Black Tea leaf extracts. *Colloids and Surfaces B: Biointerfaces* **2009,** *71*, 113-118.
53. Santhoshkumar, T.; Rahuman, A. A.; Rajakumar, G.; Marimuthu, S.; Bagavan, A.; Jayaseelan, C.; Zahir, A. A.; Elango, G.; Kamaraj, C., Synthesis of silver nanoparticles using Nelumbo nucifera leaf extract and its larvicidal activity against malaria and filariasis vectors. *Parasitology Research* **2011,** *108*, 693-702.
54. Gole, A.; Dash, C.; Ramakrishnan, V.; Sainkar, S. R.; Mandale, A. B.; Rao, M.; Sastry, M., Pepsin−Gold Colloid Conjugates: Preparation, Characterization, and Enzymatic Activity. *Langmuir* **2001,** *17*, 1674-1679.
55. Sanghi, R.; Verma, P., Biomimetic synthesis and characterisation of protein capped silver nanoparticles. *Bioresour Technol* **2009,** *100*, 501-4.
56. Shrivastava, S.; Bera, T.; Roy, A.; Singh, G.; Ramachandrarao, P.; Dash, D., Characterization of enhanced antibacterial effects of novel silver nanoparticles. *Nanotechnology* **2007,** *18*, 225103.
57. Shim, D.; Wechsler, D. S.; Lloyd, T. R.; Beekman Iii, R. H., Hemolysis following coil embolization of a patent ductus arteriosus. *Catheterization and Cardiovascular Diagnosis* **1996,** *39*, 287-290.
58. Singhal, J. P.; Ray, A. R., Synthesis of blood compatible polyamide block copolymers. *Biomaterials* **2002,** *23* , 1139-1145.
59. Ashokkumar, T.; Prabhu, D.; Geetha, R.; Govindaraju, K.; Manikandan, R.; Arulvasu, C.; Singaravelu, G., Apoptosis in liver cancer (HepG2) cells induced by functionalized gold nanoparticles. *Colloids and Surfaces B: Biointerfaces* **2014,** *123*, 549-556.
60. Raju, J.; Patlolla, J. M. R.; Swamy, M. V.; Rao, C. V., Diosgenin, a Steroid Saponin of Trigonella foenum graecum (Fenugreek), Inhibits Azoxymethane-Induced Aberrant Crypt Foci Formation in F344 Rats and Induces Apoptosis in HT-29 Human Colon Cancer Cells. *Cancer Epidemiology Biomarkers & Prevention* **2004,** *13*, 1392-1398.
61. Sun, H.; Wu, L.; Gao, N.; Ren, J.; Qu, X., Improvement of Photoluminescence of Graphene Quantum Dots with a Biocompatible Photochemical Reduction Pathway and Its Bioimaging Application. *ACS Applied Materials & Interfaces* **2013,** *5*, 1174-1179.
62. Beato-López, J. J.; Fernández-Ponce, C.; Blanco, E.; Barrera-Solano, C.; Ramírez-del-Solar, M.; Domínguez, M.; García-Cozar, F.; Litrán, R., Preparation and Characterization of Fluorescent CdS Quantum Dots used for the Direct Detection of GST Fusion Proteins. *Nanomaterials and Nanotechnology* **2012,** *2*, 10.
63. Sathyamoorthy, R.; Sudhagar, P.; Chandramohan, S.; Pal, U., Size Effect on the Physical Properties of CdS Thin Films Prepared by Integrated Physical-Chemical Approach. *Journal of nanoscience and nanotechnology* **2008,** *8*, 6481-6486.

64. Hu, F. X.; Neoh, K. G.; Kang, E. T., Synthesis and in vitro anti-cancer evaluation of tamoxifen-loaded magnetite/PLLA composite nanoparticles. *Biomaterials* **2006,** *27*, 5725-5733.
65. Ruan, J.; Song, H.; Qian, Q.; Li, C.; Wang, K.; Bao, C.; Cui, D., HER2 monoclonal antibody conjugated RNase-A-associated CdTe quantum dots for targeted imaging and therapy of gastric cancer. *Biomaterials* **2012,** *33*, 7093-7102.
66. Yong, K.-T.; Swihart, M. T., In vivo toxicity of quantum dots: no cause for concern? *Nanomedicine* **2012,** *7*, 1641-1643.
67. Hauck, T. S.; Anderson, R. E.; Fischer, H. C.; Newbigging, S.; Chan, W. C. W., In vivo Quantum-Dot Toxicity Assessment. *Small* **2010,** *6*, 138-144.
68. Gustafson, H. H.; Holt-Casper, D.; Grainger, D. W.; Ghandehari, H., Nanoparticle uptake: The phagocyte problem. *Nano Today* **2015,** *10*, 487-510.
69. Oh, E.; Liu, R.; Nel, A.; Gemill, K. B.; Bilal, M.; Cohen, Y.; Medintz, I. L., Meta-analysis of cellular toxicity for cadmium-containing quantum dots. *Nature Nanotechnology* **2016,** *11*, 479.
70. Chen, G.; Yi, B.; Zeng, G.; Niu, Q.; Yan, M.; Chen, A.; Du, J.; Huang, J.; Zhang, Q., Facile green extracellular biosynthesis of CdS quantum dots by white rot fungus Phanerochaete chrysosporium. *Colloids and surfaces. B, Biointerfaces* **2014,** *117*, 199-205.

SYNOPSIS

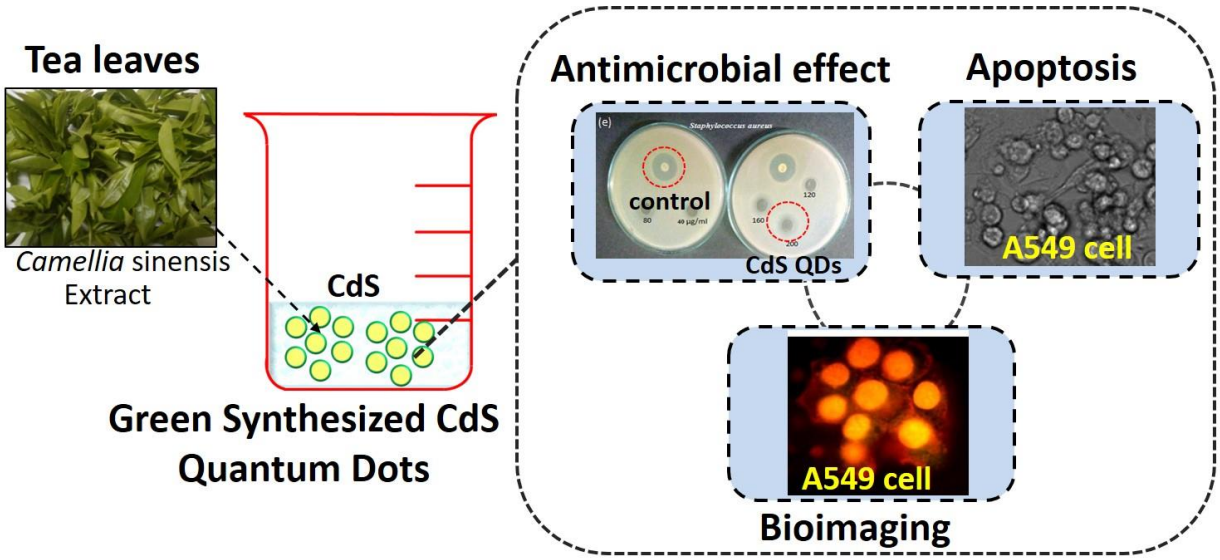
Tea leaves
Camellia sinensis
Extract
CdS
Green Synthesized CdS
Quantum Dots
Antimicrobial effect
Apoptosis
control
CdS QDs
A549 cell
A549 cell
Bioimaging